Gemi ve Deniz Teknolojisi Dergisi
Sayı: xxx, Ay Yıl
ISSN: 1300-197, e-ISSN: 2651-530X, Dergi ana sayfası: http://www.gmoshipmar.org/

DTMB 5512 İÇİN DÜZENLİ DALGALARDA, LİNEER OLMAYAN SAYISAL PARAMATERİK YALPA ANALİZİ

Fikret Dündar [1] , Ferdi Çakıcı [2]

[1]fikret.dundar@std.yildiz.edu.tr, 0009-0001-2468-7244

[2](Sorumlu Yazar), fcakici@yildiz.edu.tr, 0000-0001-9752-1125

[1,2] YILDIZ TECHNICAL UNIVERSITY, ISTANBUL, TURKIYE

TURKISH ABSTRACT

Parametrik yalpa, saniyeler içinde gelişen ve yüksek yalpa açılarına ulaşabilen tehlikeli bir fenomendir. Bu fenomen, geminin baştan veya kıçtan gelen dalgalarda seyrederken karşılaşma frekansının doğal yalpa frekansının iki katı olduğu durumlarda ve sönümün yetersiz kaldığı koşullarda ortaya çıkabilir. Geminin periyodik stabilite değişimi, mürettebat ve gemi güvenliğini tehlikeye atan, 25 dereceyi aşan yalpa açılarına neden olabilir. Bu durum aynı zamanda geminin operasyonel yeterliliğini de tehdit eder. Bu nedenle, bir savaş gemisi formu olan DTMB 5512 için parametrik yalpa analizi gerçekleştirilmiştir. Modelde aynı zamanda yalpa omurgası da mevcuttur.

Sönüm katsayılarının hesabı için Himeno'nun metodu kullanılmıştır. Farklı model hızları ve başlangıç açılarına sahip Roll Decay deneyleri incelenmiştir. Bu yöntemle, deney verilerinden lineer ve lineer olmayan sönüm katsayıları elde edilmiştir. Ayrıca, benzer gemi geometrilerinde kullanılabilmesi amacıyla boyutsuz sönüm katsayıları elde edilmiştir.

GM değerlerinin hesaplanması ve GZ eğrisinin elde edilmesinde Maxsurf Stabilty adlı paket program kullanılmıştır. Python programlama dili kullanılarak Runge Kutta metodu kodlanmış ve nümerik analiz bu şekilde gerçekleştirilmiştir. On farklı dalga yüksekliğinde, yirmi dört farklı hız senaryosunda toplamda iki yüz kırk analiz yapılmıştır. Her senaryo için maksimum yalpa açısı belirlenmiştir. Özellikle karşılaşma frekansının doğal yalpa frekansının iki katına yakın olduğu durumlarda yalpa açısının arttığı gözlemlenmiştir.

Analiz sonuçlarına göre maksimum yalpa açıları 25 dereceyi geçmediği için DTMB 5512 modelinin parametrik yalpa açısından hassas olmadığı belirlenmiştir.

Keywords: DTMB 5512, Parametrik Yalpa, Sönüm, Roll Decay

GMO Journal of Ship and Marine Technology Journal
Volume: xxx, Month Year
ISSN: 1300-1973, e-ISSN: 2651-530X, Journal homepage: http://www.gmoshipmar.org/

NON-LINEAR NUMERIC PARAMETRIC ROLL ANALYSIS OF THE DTMB 5512 IN REGULAR WAVES

Fikret Dündar [1] , Ferdi Çakıcı [2]

[1]fikret.dundar@std.yildiz.edu.tr, 0009-0001-2468-7244

[2](Corresponding author), fcakici@yildiz.edu.tr, 0000-0001-9752-1125

[1,2] YILDIZ TECHNICAL UNIVERSITY, ISTANBUL, TURKIYE

ENGLISH ABSTRACT

Parametric roll motion is a phenomenon that occurs within seconds, and it can reach high roll degrees. This phenomenon occurs when the ship is sailing in the head or following waves where the encounter frequency is twice the natural roll frequency, the wavelength is close to the ship's length, and the damping is insufficient. The periodic stability change of the vessel can cause roll angles over 25 degrees, threatening the safety of the crew and the ship. This also threatens the operational skills of the ship. Therefore, a parametric roll analysis was performed for the navy combatant model DTMB 5512. The model also has a bilge keel.

Himeno's method was employed to calculate damping coefficients based on roll decay experiments conducted at various model speeds and initial angles. This approach facilitated the extraction of both linear and non-linear damping coefficients from experimental data. Furthermore, dimensionless damping coefficients were derived to enhance applicability to similar ship geometries.

Maxsurf Stability software was utilized to compute GM values and generate the GZ curve. A Runge-Kutta method implementation in Python enabled numerical analysis, comprising a total of 240 simulations across 10 wave heights and 24-speed scenarios. For each scenario, the maximum roll angle was determined. It was observed that roll angles increased notably when the encounter frequency approached twice the natural roll frequency.

Based on the analysis findings, maximum roll angles did not exceed 25 degrees, indicating that the DTMB 5512 model is not susceptible to parametric roll resonance.

Keywords: DTMB 5512, Parametric Roll Resonance, Damping, Roll Decay

1. Introduction

Parametric roll motion is a rapid phenomenon characterized by high roll angles (exceeding 25 degrees) occurring within seconds. Research on parametric roll began in the 1930s, marked by seminal theoretical analyses by Watanabe (1934) and Kempf (1938). Subsequent studies integrated nonlinear damping and Mathieu-type equations, notably by Kerwin (1955) and Paulling and Rosenberg (1959). Experimental investigations by Paulling in 1972 further contributed to understanding this phenomenon. The practical significance of parametric roll gained prominence in the 1990s following accidents, such as the damage to a post-panamax C11 type cargo ship in 1998, which prompted detailed publications emphasizing its importance (France et al., 2003). Bulian (2004) explored the nonlinear damped 1-degree-of-freedom motion associated with the parametric roll. The International Maritime Organization (IMO) included parametric roll in the second-generation stability criteria for ship safety (Umeda, 2013), while recent studies continue to investigate various aspects of parametric roll (Cakici, 2019; Çopuroğlu et al., 2023; Luyth, 2023).

Parametric roll analysis plays a critical role in maritime safety guidelines established by classification societies such as ClassNK (2023) and ABS (2019), as well as the updated guidelines from the International Maritime Organization (IMO) in 2020. The metacentric height (GM) is a pivotal factor in parametric roll analysis, varying with different loading conditions. Recent research has explored computational fluid dynamics (CFD) solutions tailored to specific vessel types, including fishing boats (Incecik et al., 2024).

In this study, we conducted numerical parametric roll analysis specifically for the DTMB 5512 model. Damping coefficients were derived using roll decay data specific to the DTMB 5512, as detailed by Irvine et al. (2004). Both linear and nonlinear damping coefficients were considered, adhering closely to IMO guidelines. The restoring term GZ was modeled using a seventh-degree equation, while GM was approximated using a cosine function. The numerical analysis was executed utilizing the Runge-Kutta method.

2. Physical background

Parametric roll can occur when the ship's length and the wavelength of encountered waves are closely aligned, and the wave encounter frequency is twice the ship’s natural roll frequency. Changes in transverse inertia in the head or following seas lead to fluctuations in GM (metacentric height).

Ships typically have a wider beam at upper decks, especially in cargo ships, where the underwater portion is streamlined compared to the above-water structure. Consequently, when the wave trough is amidships, the ship experiences greater inertia, enhancing its stability. Conversely, when the wave crest is amidships, the ship encounters less inertia, resulting in decreased stability. The variation in GM mentioned above is influenced by factors such as wavelength, wave height, and the position of the wave. Figures 1 and 2 illustrate the submerged portions of the ship at different wave positions.

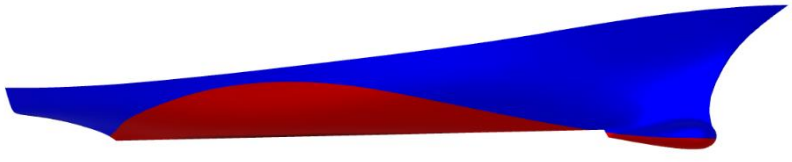

Figure 1. View of the DTMB 5512 when the ship is on the wave crest

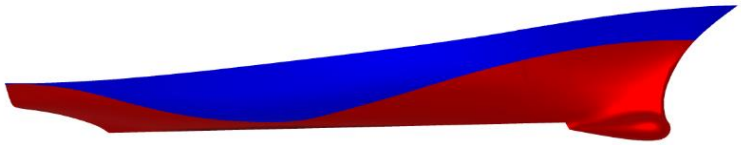

Figure 2. View of the DTMB 5512 when the ship is on the wave trough

Figure 3 and Figure 4 depict the submerged waterplane area of the ship at various positions relative to the wave. These perspectives should be considered together for a comprehensive evaluation. Equations 1 and 2 illustrate that dividing transverse inertia by displacement provides the BM value. The volume of displacement and the vertical distance to the center of gravity remain constant. Equation 3 highlights that inertia depends on the height and width of the submerged part of the ship. As the wave moves past the ship, the relationship with width becomes crucial, especially as the height varies at different points along the ship. The variation of these two variables relative to the wave's position defines the changes in GM.

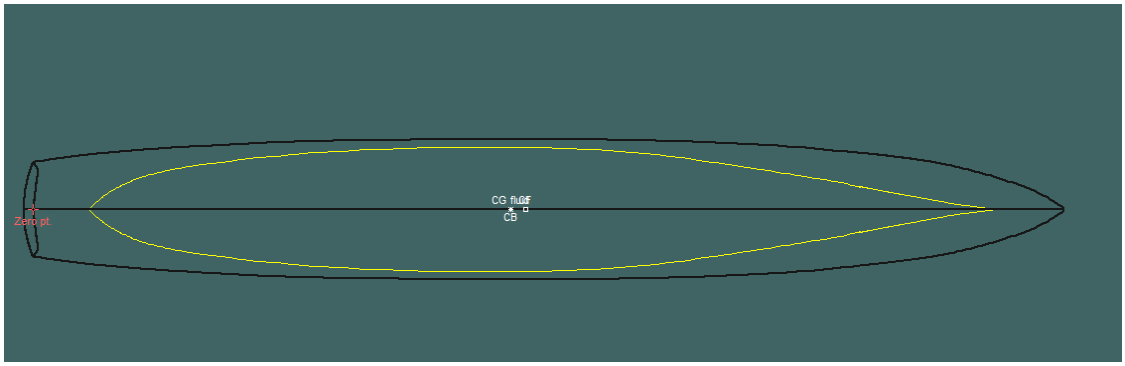

Figure 3. Waterplane area view of the DTMB 5512 when the ship is on the wave crest

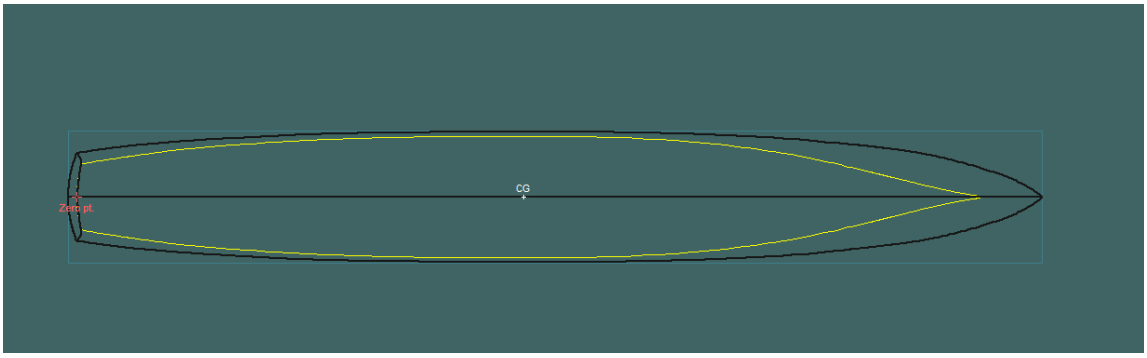

Figure 4. Waterplane area view of the DTMB 5512 when the ship is on the wave trough

Parametric roll is characterized by periodic changes influenced by the relationship between the ship's natural roll frequency and the encounter frequency of waves. Figure 5 illustrates a scenario where the encounter frequency is twice the ship's natural roll frequency. Initially, at the zero-roll degree point with the wave crest position, the ship experiences zero roll angle. As the wave progresses, the ship reaches its maximum roll angle with the wave in a trough position. During this phase, the ship's stability is enhanced due to a greater restoring moment. Subsequently, as the ship continues to roll, the wave position returns to a crest. At this stage, the ship's stability decreases, leading to increased rolling compared to earlier stages. Following this, the ship reaches its maximum roll angle again when the wave returns to a trough position. Consequently, stability improves once more. This cyclic pattern of roll and stability changes is characteristic of parametric roll phenomena, influenced by the dynamic interplay between wave conditions and the ship's response.

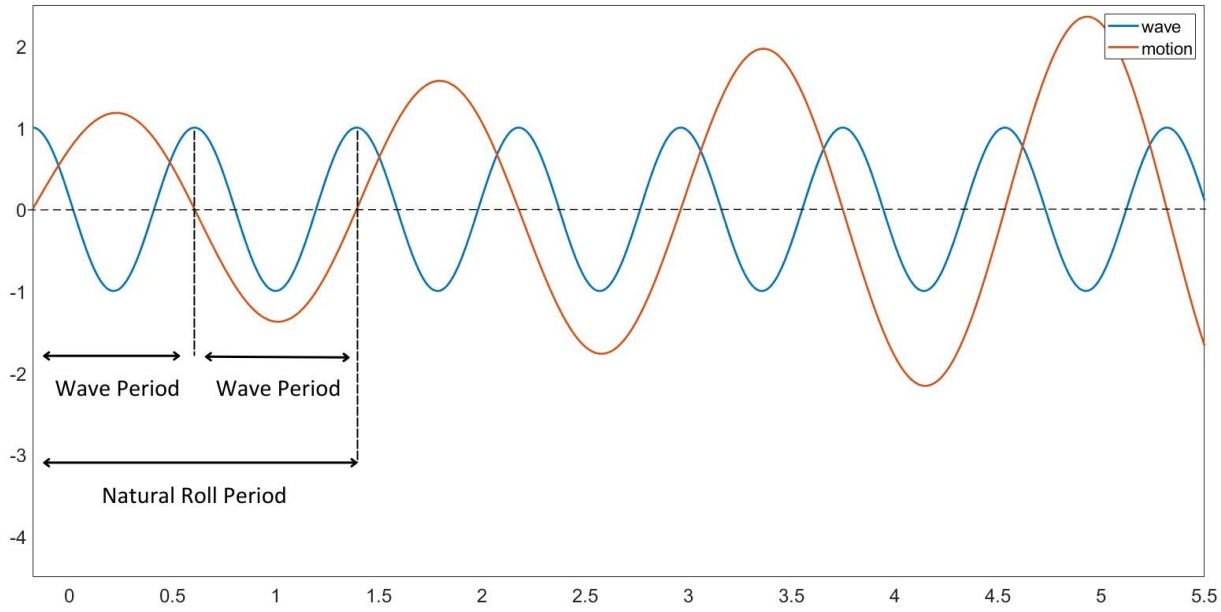

Figure 5. Sample wave profile

According to Luthy (2023), the following conditions are required for parametric roll to occur:

- Wavelength should be close to the length of the ship
- GM value should be affected as much as possible by the interaction of the hull of the ship with the wave profile
- Encounter frequency should be twice the natural roll frequency of the ship
- Head or following seas
- Insufficient damping

3. The method of analysis

3.1. General information about analysis

Table 1. Ship data of DTMB 5512

Symbol	Unit	Value
L_{PP}	m	3.048
L_{WL}	m	0.052
B_{WL}	m	0.409
C_B	-	0.506
T	m	0.132
Displacement	N	843.66
KG	m	0.163
GM	m	0.043
$\lambda_w = L_{WL}$	m	3.052

In many studies, it is possible to observe different values between GM and KG values. The reason why the values used here are different is due to differences in the baseline selection. In this study, the baseline is taken as Figure 6. The values are taken from *Irvine et al., 2004*. Also, it must be said that the bilge keel is also present on hull.

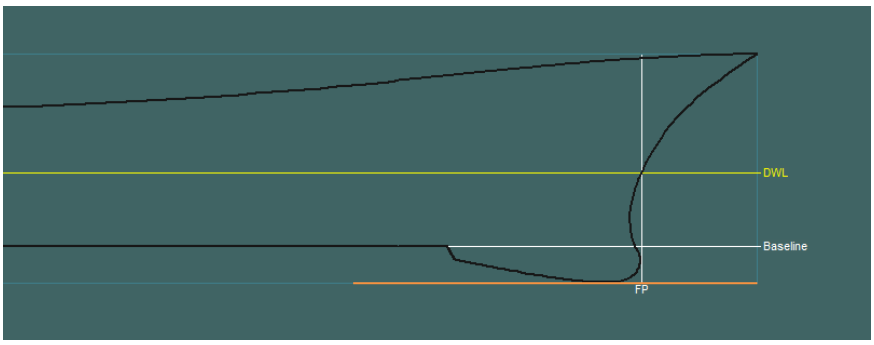

Figure 6. Baseline selection

It is possible to see the equation of roll motion in various forms. In this study, a roll equation has dynamic GZ term, linear and non-linear (third degree) damping coefficient terms. Each part of the equation will be explained in the following sections. Briefly, the Mathieu-Type is in Equation 1 if the ship is sailing in longitudinal seas, there is no wave heeling moment:

$$(I_{44} + A_{44})\ddot{\phi} + B_{44}\dot{\phi} + \Delta GM(t)\phi = 0 \tag{1}$$

B_{44} is the linear or linearized damping coefficient. In this study, a non-linear damping coefficient will be used. $\Delta GM(t)\phi$ is the restoring moment. At the lower roll degrees, $GM(t)\phi$ can be used but parametric roll resonance reaches high roll degrees and this formula can not be used in this situation. Also, the Mathieu equation can only indicate whether parametric rolling has started or not. At the high roll degrees, the solution goes to infinite. Therefore Mathieu equation is insufficient to find the final degree of parametric roll resonance. So, $GZ(\phi, t)$ can be used to better express the restoring moment at high roll degrees. After this adjustment, the equation becomes the following:

$$(I_{44} + A_{44})\ddot{\phi} + B_{44L}\dot{\phi} + B_{44NL}\dot{\phi}^3 + \Delta GZ(\phi, t) = 0 \tag{2}$$

3.2. Restoring Term

$$GZ(\phi, t) = [GM_m + GM_a \cos(\omega_e * t)][a\phi^7 + b\phi^5 + c\phi^3 + d\phi] \tag{3}$$

The restoring term is expressed as Equation 3 (Cakici, 2019). As seen, GZ is a function that has different parameters. "GM_{max} and GM_{min} are maximal and minimal instantaneous values of GM for several wave crest positions along the ship hull."(Belenky et al.,2011)

$$GM_m = 0.5(GM_{max} + GM_{min}) \tag{4}$$

$$GM_a = 0.5(GM_{max} - GM_{min}) \tag{5}$$

Also, wave height is defined as follows [4]:

$h_j = 0.01 * jL\,, \qquad where\ j = 0,1,2,3 \dots 9,10$

Table 2 shows GM_m and GM_a values for different wave heights calculated with the help of the Maxsurf Stability. The wave heights listed in the Table 2 are 0.065 meters less than the actual values. This is because the baseline has been chosen as the reference point. The distance of 0.065 meters is the gap between the baseline and the orange line seen in Figure 6.

Table 2. GM_m, GM_a, and wave height values

H	0.024	0.048	0.072	0.096	0.120	0.144	0.168	0.192	0.216	0.240
GM_a	0.0025	0.0050	0.0085	0.0085	0.0100	0.0120	0.0120	0.0465	0.0480	0.0485
GM_m	0.0425	0.0420	0.0415	0.0425	0.0430	0.0440	0.0450	0.0155	0.0180	0.0185

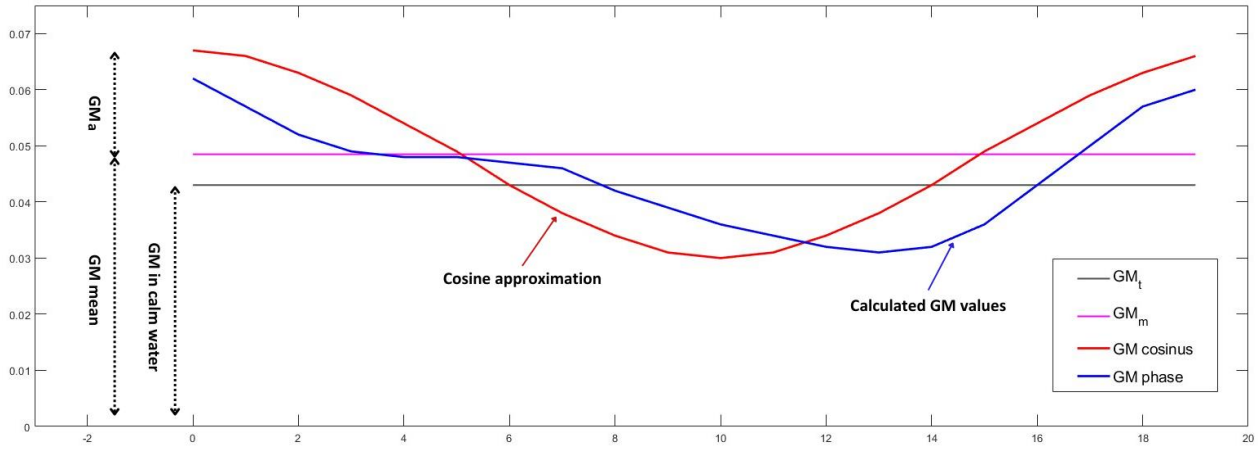

Figure 7. Cosine function of GM values

To make it easier to express the GM changing with the position of the wave, the encounter frequency and time are used. An example result is shown in Figure 7. The curves in Figure 7, are calculated for DTMB 5512 and show an example cosine approximation for DTMB 5512.

To find a,b,c, and d coefficients, the GZ graph was obtained with the help of the maxsurf stability software. Then GZ values were divided by GM_T value. Using Matlab, a curve was fitted for GZ/GM_T values by the form in Equation 7. The fitted curve can be seen in Figure 8. The a,b,c, and d coefficients obtained as a result of curve fitting are as in Table 3.

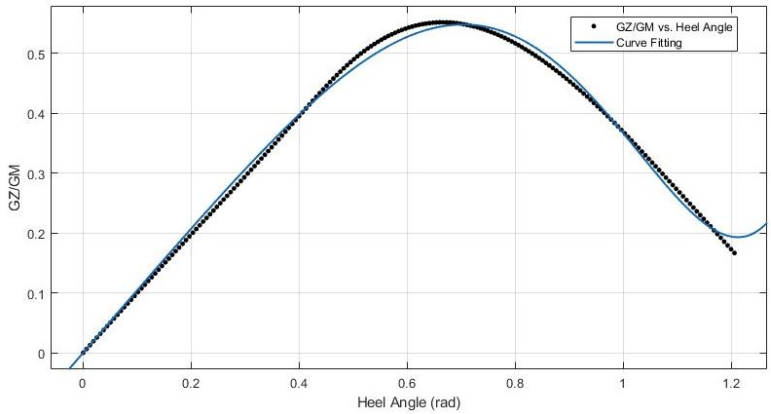

Figure 8. GZ curve fitting

Table 3. GZ coefficients

Symbol	Value
a	0.4518
b	-0.9550
c	-0.1745
d	1.0440

3.3. Mass moment of inertia and virtual mass moment of inertia

As stated in Equation 10, a restoring term and model natural roll period are needed to find inertia and added inertia. The restoring term was calculated with the help of Equation 11. When the roll decay results of the model are examined, different natural roll periods are observed at different speeds and initial angles. The natural roll period was calculated at all speeds and initial angles. As seen in Table 4, a natural roll period was obtained with the average of these values.

$$T_\phi = 2\pi * \sqrt{\frac{I_{44} + A_{44}}{C_{44}}} \tag{6}$$

$$C_{44} = \Delta * GM \tag{7}$$

Table 4. Froude numbers, initial angles, and natural roll periods

Fn	10 Degree	15 Degree	20 Degree	Mean
0.069	1.610	1.616	1.629	1.618
0.096	1.615	1.621	1.622	1.619
0.138	1.613	1.615	1.617	1.615
0.190	1.599	1.603	1.609	1.604
0.280	1.579	1.585	1.583	1.582
0.340	1.550	1.559	1.562	1.557
0.410	1.531	1.520	1.543	1.531
			Total mean:	1.590

The average inertia of the ship was found using the average natural period and restoring term.

$$I_{44} + A_{44} = 2.322 \quad \text{kg} * m^2$$

3.4. Damping Coefficients

Equation 8 is the general formula for the damping coefficients. In this study, the B_2 term will be ignored since the damping coefficient with a 2nd order term will not be used. In the rest of the study, B_L will stand for B_1 as it represents the linear coefficient. B_{NL} will also be used for the B_3.

$$\Delta\emptyset = \frac{\pi}{2}\frac{\omega_\emptyset}{C_{44}}\,\emptyset_m\,[B_1 + \frac{8}{3\pi}\omega_\emptyset\emptyset_m B_2 + \frac{3}{4}\omega_\emptyset^2\emptyset_m^2 B_3] \tag{8}$$

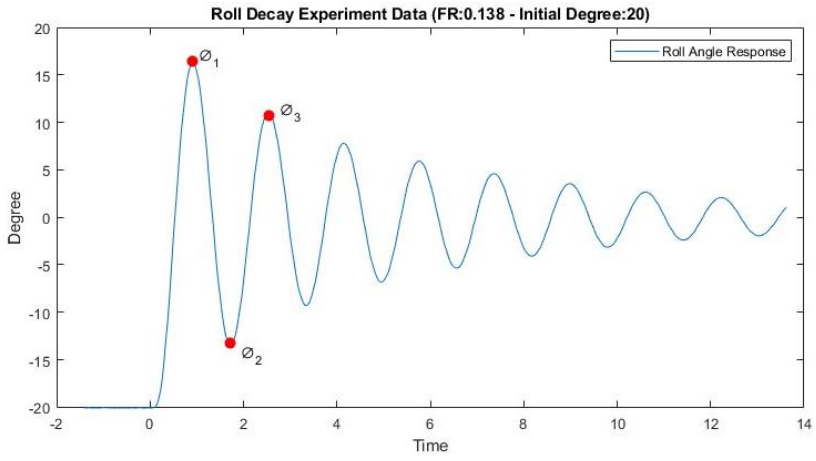

Figure 9. Roll Decay Curve

To determine the damping coefficients, roll decay test data were analyzed across all speeds and initial angles of 10°, 15°, and 20°. Given the intention to incorporate non-linear damping coefficients in the study, Himeno's method, as described by Himeno (1981), was employed. This method is specifically suited for extracting non-linear damping characteristics from experimental data, ensuring accurate characterization of the ship's damping behavior during roll decay tests. In experimental data, as in Figure 9, the points where the roll degree of the model peaks are determined. Using Equations 9 and 10, the difference between the peak points and after that, the averages of the peak points are calculated.

$$\Delta\emptyset = \emptyset_{n-1} - \emptyset_n \tag{9}$$

$$\emptyset_m = \frac{\emptyset_{n-1} + \emptyset_n}{2} \tag{10}$$

Table 5. An example of peaks determination (Fn:0.138, initial degree: 20)

i	0	1	2	3	4	5	6	7	8	9	10
Degree	-20.000	16.243	-13.403	10.997	-9.276	7.781	-6.817	5.919	-5.342	4.591	-4.093
Radian	-0.349	0.283	-0.234	0.192	-0.162	0.136	-0.119	0.103	-0.093	0.080	-0.071
Φ_m	0.316	0.259	0.213	0.177	0.149	0.127	0.111	0.098	0.087	0.076	0.067
$\Delta\Phi$	0.066	0.050	0.042	0.030	0.026	0.017	0.016	0.010	0.013	0.009	0.010

After calculating $\emptyset_m$ *and* $\Delta\emptyset$ values, a curve fitting was performed using Matlab software. In Figure 10, the curve fitting using peak values can be seen. With the equation obtained with the curve, Equation 12 can be equated. This can be seen in Equation 15. The transformation in Equation 11 is used for the restoring term (C_{44}). With the modifications made to the equation 15, B_L *and* B_{NL} are obtained in Equation 16 and 17.

The process in Figure 10 was performed for each speed and initial angle. Table 6 shows the values of k_1 and k_3.

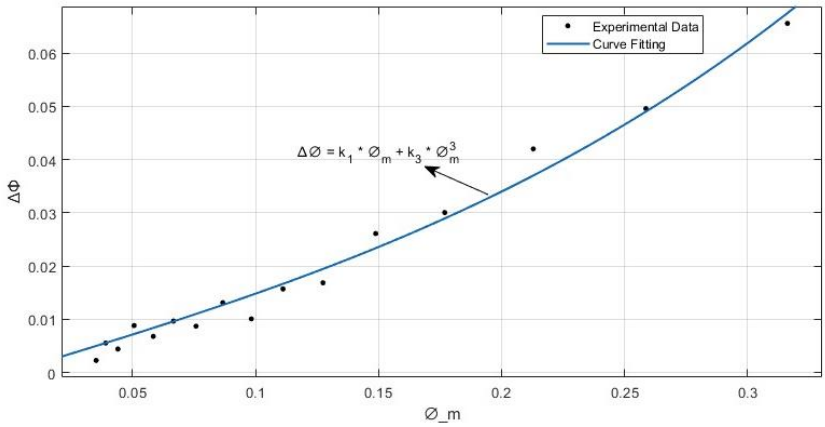

Figure 10. Curve fitting Φ_m - $\Delta\Phi$

$$k_1\emptyset_m + k_3\emptyset_m^3 = \frac{\pi}{2}\frac{\omega_\emptyset}{C_{44}}\emptyset_m B_L + \frac{\pi}{2}\frac{\omega_\emptyset}{C_{44}}\emptyset_m\frac{3}{4}\omega_\emptyset^2\emptyset_m^2 B_{NL} \tag{15}$$

$$B_L = \frac{(k_1 * 2 * \Delta * GM)}{\pi * \omega_\emptyset} \tag{16}$$

$$B_{NL} = \frac{(k_3 * 8 * \Delta * GM)}{3 * \pi * {\omega_\emptyset}^3} \tag{17}$$

Table 6. Froude numbers with k_1 and k_3, B_L and B_{NL} values

	10 Degree		15 Degree		20 Degree		Mean		Mean	
Fn	K_1	K_3	K_1	K_3	K_1	K_3	K_1	K_3	B_{NL}	B_L
0.069	0.0852	0.7934	0.0925	0.6461	0.0964	0.6273	0.0914	0.6889	0.3124	0.5172
0.096	0.0735	2.4241	0.0865	1.2270	0.0885	1.0079	0.0828	1.5530	0.7041	0.4689
0.138	0.1231	2.3301	0.1266	1.4163	0.1316	1.0453	0.1271	1.5972	0.7242	0.7195
0.190	0.1888	-0.1952	0.1821	0.6285	0.1814	0.6407	0.1841	0.3580	0.1623	1.0421
0.280	0.1912	2.8576	0.2042	1.3570	0.2220	0.4862	0.2058	1.5669	0.7104	1.1649
0.340	0.2178	2.8760	0.2292	1.4073	0.2403	0.8342	0.2291	1.7058	0.7734	1.2968
0.410	0.2980	0.4669	0.2926	0.9056	0.2971	0.4596	0.2959	0.6107	0.2769	1.6750

The relation of the non-dimensional damping coefficient can be seen in Equation 18. “a, b, c” is called the decay coefficient or extinction coefficient. In our equation, it corresponds to K_1, K_2, K_3. With the help of this equation, the relation between ship speed and non-dimensional damping coefficient can be seen in Table 7.

$$2\alpha = a\frac{2}{\pi}\omega_{\emptyset}$$
$$\beta = b\frac{3}{4}\frac{180}{\pi} \tag{18}$$
$$\gamma = c\frac{8}{3\pi\omega_{\emptyset}}\left(\frac{180}{\pi}\right)^2$$

Table 7. Non-dimensional damping coefficients

Fn	ϒ	Ķ
0.069	470.5244	0.0582
0.096	1060.661	0.0527
0.138	1090.871	0.0809
0.190	244.5051	0.1172
0.280	1070.177	0.1310
0.340	1165.042	0.1458
0.410	417.0930	0.1884

After these calculations, a scatter plot was drawn with speed (m/s) on the x-axis and linear or non-linear damping coefficients on the y-axis. As can be seen in Figures 11 and 12, a 2nd order curve fitting was performed for the linear coefficient, while a 1st order curve fitting was performed for the non-linear damping coefficient. Thus, the relationship between damping coefficient and speed was revealed for DTMB 5512.

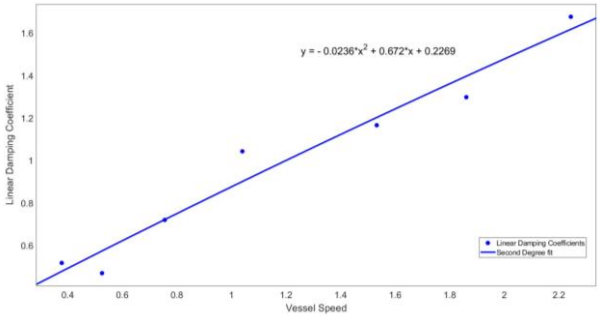

Figure 11. Linear coefficient – ship speed (m/s)

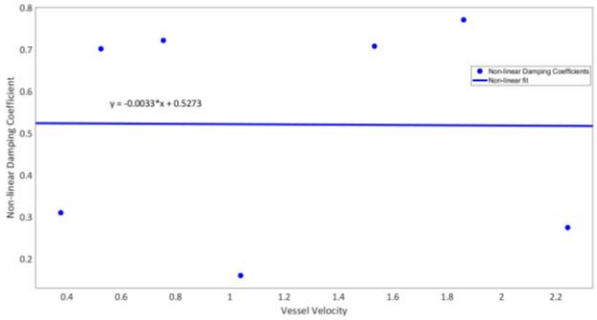

Figure 12. Non-linear coefficient – ship speed (m/s)

3.5. Numerical Analysis Background

Runge kutta was used for numerical analysis. Code was written in Python language to perform the analysis. First of all, Equation 6 was analyzed by the Euler method. Then Runge Kutta was compared with Euler's method. Finally, all the analysis was performed with Runge Kutta. The algorithm can be seen in Figure 13. The inputs of the algorithm are as follows:

- Speed

Table 8. Speed Coefficients

i	K_i	i	K_i
1	1.0	13	-1.0
2	0.991	14	-0.991
3	0.996	15	-0.996
4	0.924	16	-0.924
5	0.866	17	-0.866
6	0.793	18	-0.793
7	0.707	19	-0.707
8	0.609	20	-0.609
9	0.500	21	-0.500
10	0.383	22	-0.383
11	0.259	23	-0.259
12	0.131	24	-0.131

$$\omega_e = \omega - k * V * \cos(\varphi_w) \tag{19}$$

Equation 19 shows how the encounter frequency is calculated for the speed a ship has. φ_w refers to the angle of encounter. Since the ship will be examined with the head and following waves, $\varphi_w = 1\ or\ -1$. Therefore, in Table 8, $i \leq 12$ refers to follow waves, while $i > 12$ refers to head waves. The speed coefficients in the table express the ratio with service speed. The service speed of the ship is assumed to be Fn= 0.41. With the help of Equation 20, the ship's service speed at Fn= 0.41 is equal to 2.2434 m/s.

$$Fn = \frac{V}{\sqrt{g * L}} \tag{20}$$
$$V_s = 2.2434\ m/s$$

- Wave Height

Wave height as an input determines the values of GM_m and GM_a in the equation. More information on wave heights is in section 2.2.

- Initial Roll Amplitude and Roll Velocity

$$\emptyset = 0.0872\ rad\ \ (5\ degree)$$
$$\dot{\emptyset} = 0\ rad/s$$

- Time

The time interval for numerical analysis was determined as 0.01 seconds.

- Runge-Kutta Method

In the numerical analysis, the 4th-order Runge-Kutta method was used to calculate the instantaneous roll angles and velocities.

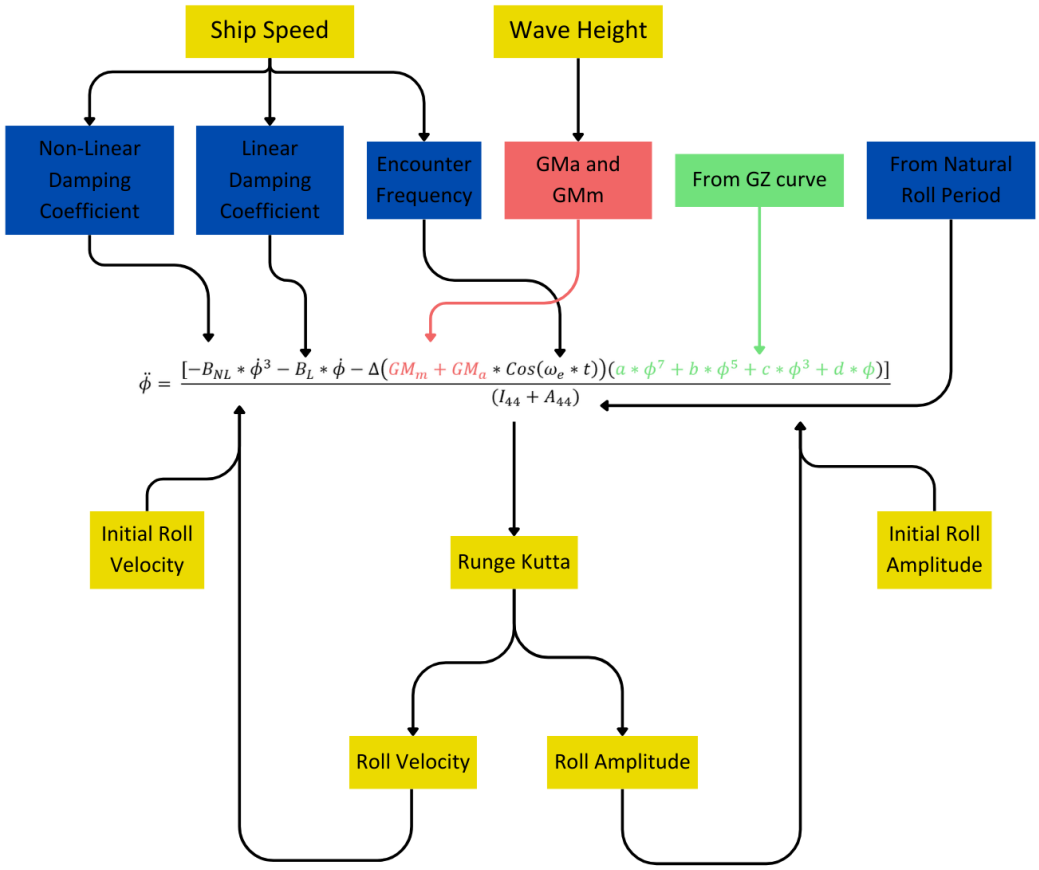

Figure 13. Algorithm of analysis

4. Calculation and graphs

4.1. Validation

To assess the proximity of the calculated damping coefficients to experimental values, the experimental results were compared with those derived from the Runge-Kutta Method. The time interval was consistently set at 0.01 seconds, and the equation was structured to depict free-damped motion. Figures 14 to 21 present a comparative analysis of the experimental outcomes and the results obtained using the Runge-Kutta method.

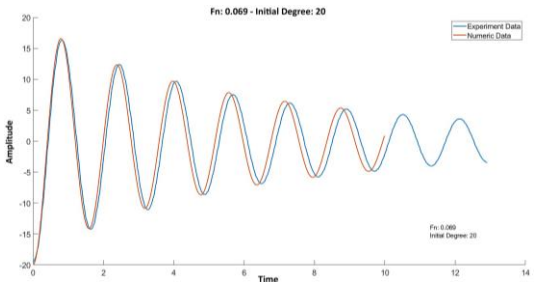

Figure 14. Fn:0.069, inital degree:20

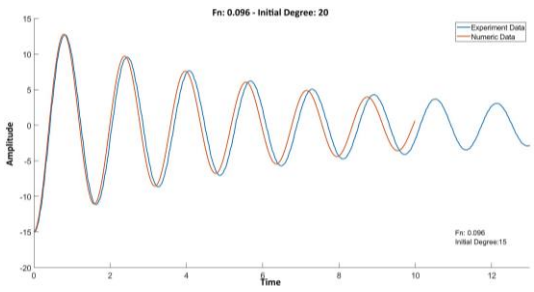

Figure 15. Fn:0.096, inital degree:15

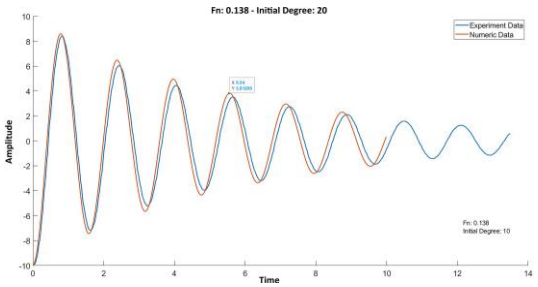

Figure 16. Fn:0.138, initial degree:10

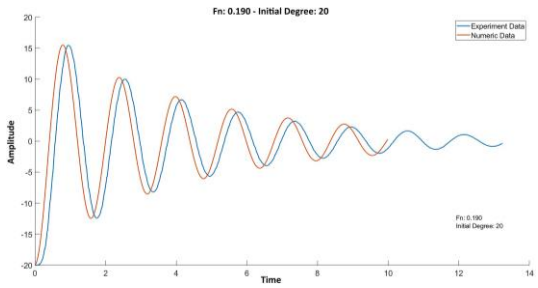

Figure 17. Fn:0.190, initial degree:20

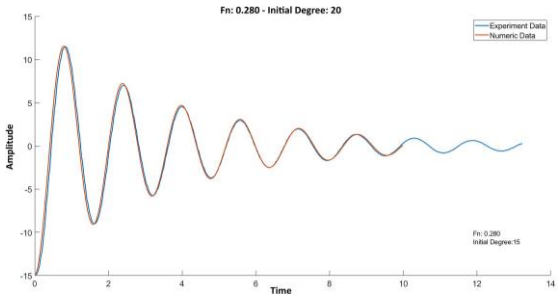

Figure 18. Fn:0.280, initial degree:15

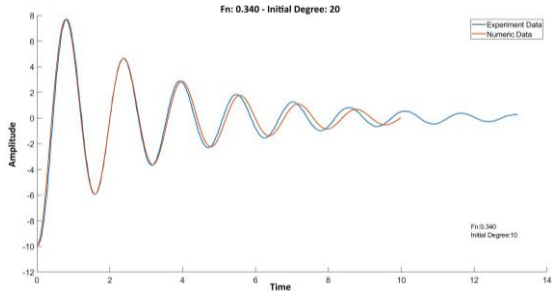

Figure 19. Fn:0.340, initial degree:10

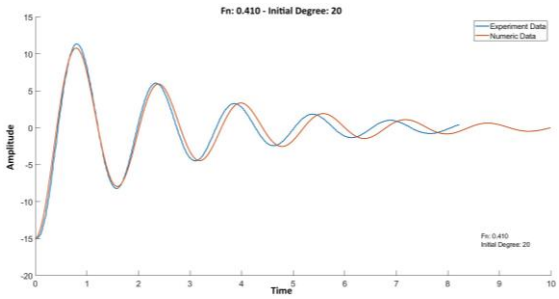

Figure 20. Fn:0.410, initial degree:15

4.2. Results

Table 9 on the subsequent pages displays the wave heights, ship speeds, encounter frequencies, and maximum roll angles (degrees). Additionally, motion graphs depicting these unstable states can be found in Figures 21 to 26.

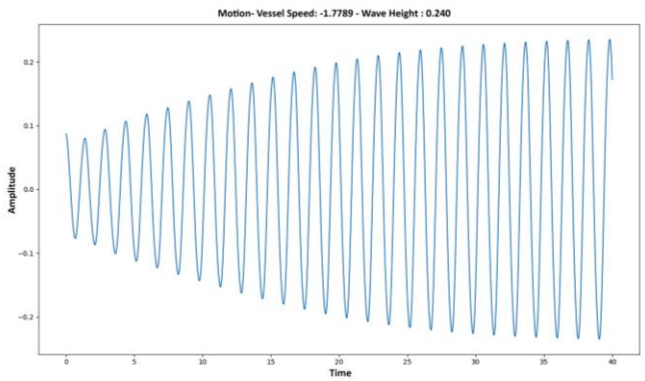

Figure 21. Speed: -1.7789 m/s – wave height: 0.24 m

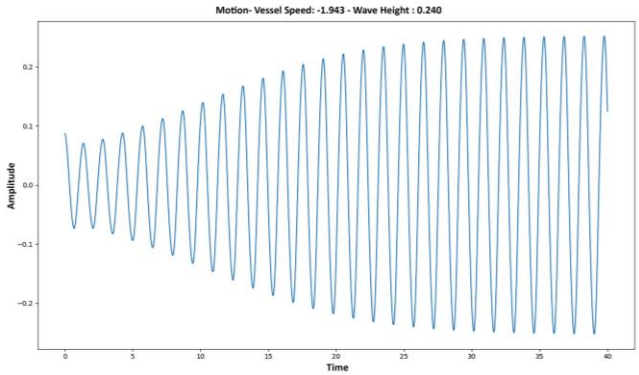

Figure 22. Speed: -1.943 m/s – wave height: 0.240 m

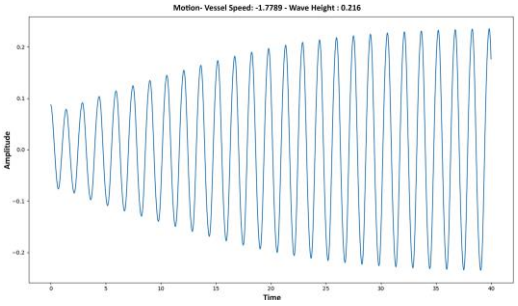

Figure 23. Speed: -1.7789 m/s – wave height: 0.216 m

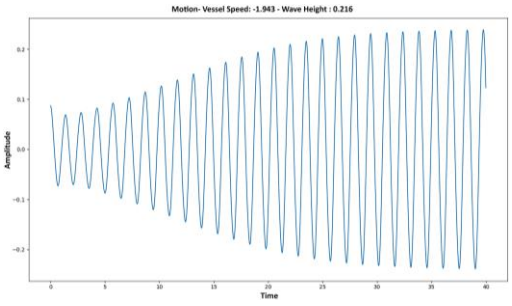

Figure 24. Speed: -1.943 m/s – wave height: 0.216 m

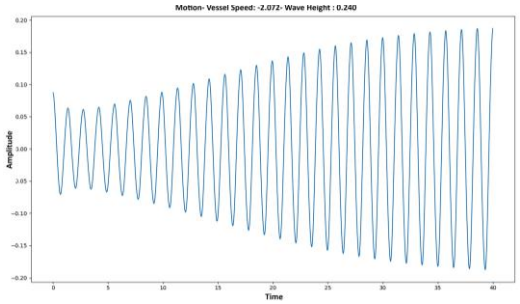

Figure 25. Speed: -2.0727 m/s – wave height: 0.240 m

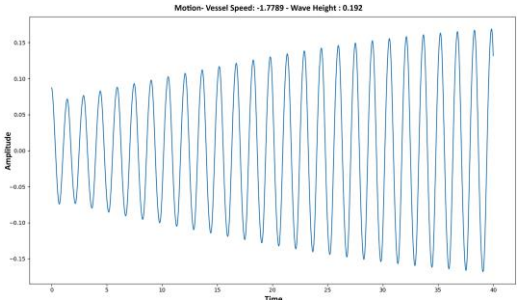

Figure 26. Speed: -1.7789 m/s – wave height: 0.192 m

Table 9. Maximum roll angle

Fn/H	m/s	0.024	0.048	0.072	0.096	0.120	0.144	0.168	0.192	0.216	0.240	ω_e	ω_e / ω_Φ
0.054	0.293	5.00	5.00	5.00	4.99	4.99	4.99	4.99	4.99	4.99	4.99	3.89	0.865
0.106	0.581	5.00	5.00	5.00	4.99	4.99	4.99	4.99	4.99	4.99	4.99	3.30	0.734
0.157	0.859	5.00	5.00	5.00	4.99	4.99	4.99	4.99	4.99	4.99	4.99	2.73	0.606
0.205	1.121	5.00	5.00	5.00	4.99	4.99	4.99	4.99	4.99	4.99	4.99	2.18	0.486
0.250	1.366	5.00	5.00	5.00	4.99	4.99	4.99	4.99	4.99	4.99	4.99	1.68	0.374
0.290	1.586	5.00	5.00	5.00	4.99	4.99	4.99	4.99	4.99	4.99	4.99	1.23	0.273
0.325	1.778	5.00	5.00	5.00	4.99	4.99	4.99	4.99	4.99	4.99	4.99	0.83	0.185
0.355	1.943	5.00	5.00	5.00	4.99	4.99	4.99	4.99	4.99	4.99	4.99	0.49	0.110
0.379	2.072	5.00	5.00	5.00	4.99	4.99	4.99	4.99	4.99	4.99	4.99	0.23	0.050
0.396	2.167	5.00	5.00	5.00	4.99	4.99	4.99	4.99	4.99	4.99	4.99	0.03	0.007
0.406	2.223	5.00	5.00	5.00	4.99	4.99	4.99	4.99	4.99	4.99	4.99	-0.08	-0.018
0.410	2.343	5.00	5.00	5.00	4.99	4.99	4.99	4.99	4.99	4.99	4.99	-0.12	-0.028
-0.054	-0.293	5.00	5.00	5.00	4.99	4.99	4.99	5.09	5.11	5.21	5.21	5.10	1.135
-0.106	-0.581	5.00	5.00	5.00	4.99	5.01	5.18	5.33	5.37	5.51	5.52	5.69	1.266
-0.157	-0.859	5.00	5.00	5.00	4.99	5.03	5.27	5.50	5.59	5.80	5.82	6.26	1.394
-0.205	-1.121	5.00	5.00	5.00	4.99	4.99	5.09	5.38	5.57	5.88	5.93	6.80	1.514
-0.250	-1.366	5.00	5.00	5.00	4.99	4.99	4.99	4.99	5.21	5.60	5.67	7.31	1.626
-0.290	-1.586	5.00	5.00	5.00	4.99	4.99	4.99	4.99	5.16	5.82	5.92	7.76	1.727
-0.325	-1.778	5.00	5.00	5.00	4.99	4.99	4.99	6.96	9.67	13.47	13.49	8.16	1.815
-0.355	-1.943	5.00	5.00	5.00	4.99	4.99	4.99	4.99	6.75	13.68	14.45	8.49	1.890
-0.379	-2.072	5.00	5.00	5.00	4.99	4.99	4.99	4.99	4.99	8.63	10.70	8.76	1.950
-0.396	-2.167	5.00	5.00	5.00	4.99	4.99	4.99	4.99	4.99	4.99	4.99	8.96	1.993
-0.406	-2.223	5.00	5.00	5.00	4.99	4.99	4.99	4.99	4.99	4.99	4.99	9.07	2.018
-0.410	-2.343	5.00	5.00	5.00	4.99	4.99	4.99	4.99	4.99	4.99	4.99	9.11	2.028

5. Conclusion

Parametric roll resonance significantly impacts the operational capabilities of naval combatants. Therefore, in the current thesis, an analysis of parametric roll resonance was conducted for the DTMB 5512 model. This analysis involved determining both linear and non-linear damping coefficients, as well as non-dimensional damping coefficients. GM values for the restoring term were established based on varying wave heights, and GZ coefficients were also calculated. Using the Runge-Kutta method for analysis, maximum roll angles were observed to reach approximately 14 degrees. Although this angle does not meet the IMO threshold of 25 degrees for considering parametric roll, it is crucial to recognize that such roll angles still pose significant risks and should be carefully evaluated.

Acknowledgments

This study is supported by project number 123M482 of the Scientific and Technological Research Council of Türkiye.

6. References

ABS (2019), "The Assessment of Parametric Roll Resonance in the Design of Container Carriers."

Bekhit, A., & Popescu, F. (2021). Uranse-based numerical prediction for the free roll decay of the DTMB ship model. Journal of Marine Science and Engineering, 9(5), 452.

Belenky, Vadim, C. Bassler, ve K. Spyrou. "Development of second generation intact stability criteria". Hydromechanics Department Report, Naval Surface Warfare Center Carderock Division-50-TR-2011/065, 2011

Bulian, G. (2004). Approximate analytical response curve for a parametrically excited highly nonlinear 1-DOF system with an application to ship roll motion prediction. Nonlinear Analysis of Real-World Application. Vol. 5, No.4 pp.725–748

Cakici, F. (2019). A Numerical Application of Ship Parametric Roll under Second Generation Stability Criteria. Journal of ETA Maritime Science, 7.

ClassNK (2023). Guidelines on Preventive Measures against Parametric Rolling (Edition 1.0)." ClassNK.

Çopuroğlu, H.I., Pesman, E., Taylan, M. (2023). Assessment of second-generation intact stability criteria and case study for a Ro-Ro ship, Proceedings of the 19th International Ship Stability Workshop, Istanbul, Türkiye, 9-11 September, pp. 315-320.

France, W.L. et al. (2003) "An Investigation of Head-Sea Parametric Rolling and Its Influence on Container Lashing Systems", Marine Technology, 40(1)

Gokce, M. K., & Kinaci, O. K. (2018). Numerical simulations of free roll decay of DTMB 5415. Ocean Engineering, 159, 539–551.

Himeno, Y. (1981). Prediction of ship roll damping-a state of the art.

IMO, H. (2020). Interim guidelines on the second generation intact stability criteria. International Maritime Organization London, UK.

International Towing Tank Conference (ITTC). (2011). "Numerical Estimation of Roll Damping". ITTC Recommended Procedures and Guidelines, 7.5-02-07-04.5.

Irvine, M., J. Longo, and F. Stern. "Towing Tank Tests for Surface Combatant for Free Roll Decay and Coupled Pitch and Heave Motions." In Proceedings of 25th ONR Symposium on Naval Hydrodynamics, St Johns, Canada, 2004.

Iqbal, M., Terziev, M., Tezdogan, T. et al. Unsteady RANS CFD Simulation on the Parametric Roll of Small Fishing Boat under Different Loading Conditions. J. Marine. Sci. Appl. **23**, 327–351 (2024).

Kerwin, J.E. (1955) “Note on Rolling in Longitudinal Waves”, International Shipbuilding Progress, 2(16), pp.597-614

Kempf, G. (1938). Die Stabilita¨t Beanspruchung der Schiffe Durch Wellen und Schwingungen. Werft Reederei Hafen, Vol.19 pp. 200–202.

Luthy, Vivien. “Probability of occurrence of parametric roll on a predefined sea state”. PhD Thesis, Paris, HESAM, 2023.

Mancini, S., Begovic, E., Day, A. H., & Incecik, A. (2018). Verification and validation of numerical modelling of DTMB 5415 roll decay. Ocean Engineering, 162, 209–223.

Paulling, J.R. and Rosenberg, R.M., "On unstable ship motions resulting from nonlinear coupling." Journal of Ship Research, Vol. 3 pp. 36–46 (1959).

Paulling, J.R., Kastner, S. and Schaffran, S., Experimental Studies of capsizing of intact ships in heavy seas, U.S. Coast Guard Technical Report, (also IMO Doc. STAB/7, 1973), (1972).

Piehl, H. (2017). Ship roll damping analysis [PhD Thesis, Dissertation, Duisburg, Essen, Universität Duisburg-Essen, 2016].

Umeda, N. 2013, "Current Status of Second Generation Intact Stability Criteria", Proceedings of the 13th International Ship Stability Workshop, Brest, pp. 138-157.

Watanabe, Y. (1934) “On the Dynamic Properties of the Transverse Instability of a Ship Due to Pitching”, Journal of the Society of Naval Architects of Japan, Vol. 53, pp.51-70, (in Japanese)